ROBUST DESIGN OPTIMIZATION OF BENCHMARK AERODYNAMIC CASE BASED ON POLYNOMIAL CHAOS EXPANSION

Huan Zhao*, Zhenghong Gao*
***School of Aeronautics, Northwestern Polytechnical University, Xi'an 710072, PR China**

Keywords: *robust design optimization (RDO), non-intrusive polynomial chaos expansion (NIPCE), uncertainty quantification (UQ), deterministic optimization*

Abstract

Transonic airfoil often shows sensitive aerodynamic performance to uncertainties of flight conditions. To build an effective design optimization method for robust transonic airfoil, The AIAA RAE2822 airfoil design optimization test case is studied by robust design optimization (RDO) method. The non-intrusive polynomial chaos expansion (NIPCE) method is applied to provide efficient and accurate uncertainty quantification (UQ). The global evolution optimization algorithm combined with surrogate model is used to build the RDO framework. As a comparison with RDO, deterministic design optimization is firstly performed and researched. These results show that deterministic optimization airfoil is often ill posed and suffering from the drastic increase of drag coefficient at off-design points, even though the drag coefficient of it at design point has been reduced by 48.42% from that of RAE 2822 airfoil. While the RDO airfoil achieves robust drag over a range of Mach numbers and improves the drag-divergence Mach number by 0.05 from RAE2822 airfoil. The case demonstrates that the proposed RDO method provide an effective approach to transonic aerodynamic optimization.

1 Introduction

The RDO method is made up of three main parts [1]. The first stage consists of identifying and quantifying the uncertain parameter associated with the problem definition and the analysis modules. Probability distribution functions (PDFs) are often used to quantifying uncertainty of these parameters. The second phase focus on the UQ through the analysis approach to obtain probabilistic descriptions of the objective functions and constraints. Robust descriptions of the objectives depend on the numerical approximation of their statistical moments including expectation and variance, and reliability forms of constraints rely on the probability the constraint is violated or exceeds a reference value. Finally, the third stage defines the mathematic model of RDO and searches for the optimal shape with robust performance. RDO for aerodynamic shape minimizes the mean and the standard deviation of objective subject to reliability constraints over the range of possible values of these uncertain parameters.

This paper focuses on building an effective RDO framework to design the robust transonic airfoil for a range of Mach number. It mainly resolves some issues as following.

Excessive computational cost and unsatisfactory accuracy are main difficulties for UQ in second stage of RDO. Existing approaches [2, 3] to UQ includes Monte Carlo simulation (MCS), Taylor-based moment propagation, numerical integral, stochastic expansion, etc. However, MCS method causes very expensive cost for UQ and usually needs at least 10^4 samples for accurate estimate of mean and variance of drag coefficient. The Taylor-based moment propagation method unless restricts the analysis to very small values of the input variance its accuracy is often unsatisfactory in the frequent case of highly nonlinear function, so that it is difficult to be used

for aerodynamic shape optimization widely. Polynomial chaos expansion (PCE) and Stochastic collocation (SC) methods are popular stochastic expansion approaches. Due to the orthogonality of polynomial terms, PCE method is a promising approach to perform this task for efficient and accurate UQ in aerodynamic shape optimization. However, applying the PCE method for UQ, the challenging problem is how to select as few collocation points as possible and proper polynomial order to obtain accurate estimate. For each of collocation points, a true value of aerodynamic performance is given to determine the unknown polynomial coefficients.

Proper mathematic model of RDO is the most critical step in the third stage of RDO. More recent RDO work only considers Mach number uncertainty and lacks reliability consideration for constraints, which is very hard to meet the design demand of the transonic airfoil. The transonic airfoil shows a strong sensitivity to Mach number, AoA, etc. For example, the performance of transonic airfoil deteriorates when lift coefficient or AOA slightly exceeds the design value, due to the occurrence of strong shocks on its surfaces[4]. Thus, the RDO problem should be formulated simultaneously considering these parameters uncertainties. Uncertainties should also be taken into account for the estimation of the constraints involved in design optimization. The constraints should be satisfied for all possible values of uncertain parameters, which is not practical for aerodynamic shape optimization problems. Alternatively, the probability of violating the constraints can be restricted within a range as small as possible, formulating the constraint in terms of reliability. The reliability constraint ensures that the optimal shape is within the feasible region of constraints with a range of tolerances. Thus, a mathematic model of RDO considering Mach number uncertainty is built subject to reliability constraints, which combines the case of transonic airfoil optimization to demonstrate the effectiveness of RDO.

The remainder of paper is organized as follows. Section. 1 presents the definition of optimization case based on AIAA aerodynamic design optimization discussion group test cases. Section. 2 builds a framework of RDO based an NIPCE method. This framework combines a global particle swarm optimization (PSO) algorithm to optimize the resulting airfoil. Section 3 presents an efficient algorithm- orthogonal matching pursuit (OMP) to construct sparse PC metamodel. Section 4 states detailed discussion and comparison of optimization results by deterministic optimization and RDO.

2 Optimization case and problem definition

The aerodynamic optimization problem comes from AIAA aerodynamic design optimization discussion group test cases [5], Eq. (1) gives the problem definition. These work about the case represent the discussions and comparisons of some single-point optimization results and make an attempt of multipoint optimization to regularize the ill-posed problem of single-point optimization. However, as we know, the difficulty of multipoint optimization is how to determine the weights and locations of points and often needs to do many tries.

$$
\begin{aligned}
& Ma = 0.734, \mathrm{Re} = 6.5\times10^{6}, C_L = 0.824 \\
& Find \quad x \in R^d \\
& Min \quad C_D \\
& S.t. \quad C_m \geq -0.092, \\
& \qquad Area \geq Initial(RAE2822),
\end{aligned} \tag{1}
$$

2.1 Deterministic optimization

In this section, we combine a global particle swarm optimization (PSO) algorithm and Kriging surrogate model to optimize the airfoil at design point. The class function/shape function transformation (CST) is used to deform the airfoil. First, we need to strike a balance among these requirements: large initial design space, refinement search in local space, and short optimization time. To circumvent this issue, we gradually increase the number of design variables at each circle. In detail, 8 variables are first used to finish the search until the drag of optimized airfoil has converged. Then, based on the result of optimization by 8 variables, 12 variables are used to continue finishing a search until the drag cannot be reduced. Next, 16 and 24 variables are used in turn to find out the optimal

result. Table 1 records the results in the optimization procedure. It is noticed that when 24 variables are used the drag coefficient has been reduced to 0.11209 with 48.42% drop to the initial value and cannot be reduced more. Fig. 1 gives the comparison of initial and optimized airfoils. Fig. 2 shows the comparison of camber distributions of these airfoils. It can be seen that the camber of optimized airfoil reduces at nearing leading edge and increases at nearing trailing edge. Fig. 3 gives the comparison of pressure distributions among these airfoils. Obviously, optimized airfoils have eliminated the shock at design point. However, as shown in Fig. 4, optimized airfoil achieves a reduction of drag coefficient only at design point so that it is very difficult to demand the requirements for engineering. That is to say that deterministic optimization airfoil is often ill posed and suffering from the drastic increase of drag coefficient at off-design points, even though the drag coefficient of it at design point has been optimized well. Therefore, in order to achieve a consistent reduction of drag coefficient over a range of Mach number, e.g., 0.65-0.75, we have to resort to RDO.

Table 1 The aerodynamic characteristics of initial and optimized airfoils at design point

Airfoil	C_D	ΔC_D	C_m	Area	CFD runs
RAE2822	0.021714	0	-0.08743	0.077870	0
8varibles	0.017621	-18.86%	-0.09060	0.077888	100
12varibles	0.012083	-44.35%	-0.09184	0.078527	200
16varibles	0.011460	-47.22%	-0.09160	0.078106	500
24varibles	0.011202	-48.42%	-0.08690	0.077918	1000

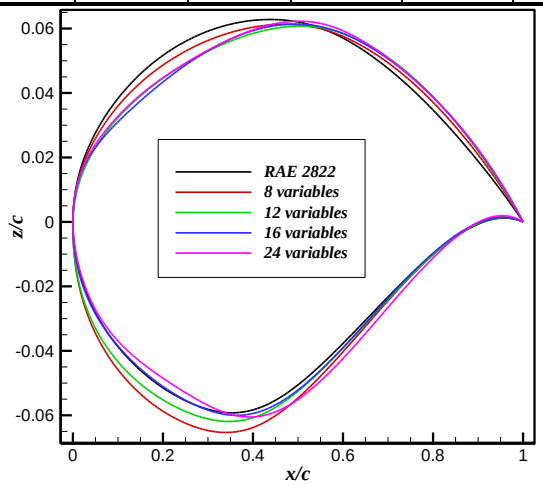

Fig. 1. Initial and optimized airfoils

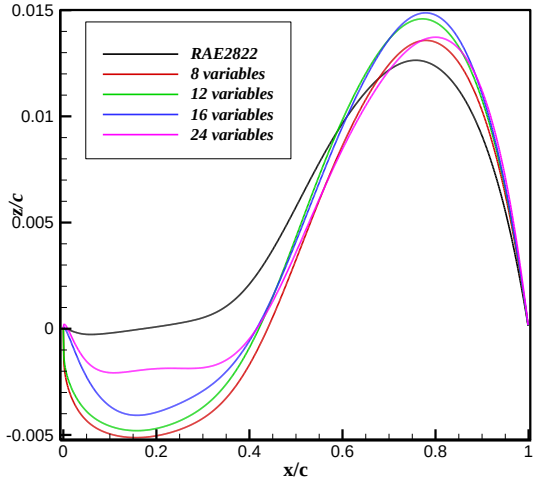

Fig. 2. Initial and optimized camber distributions of airfoils

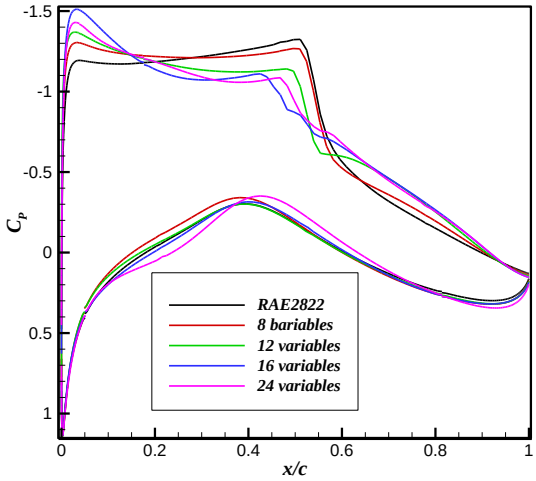

Fig. 3. Initial and optimized pressure distributions.

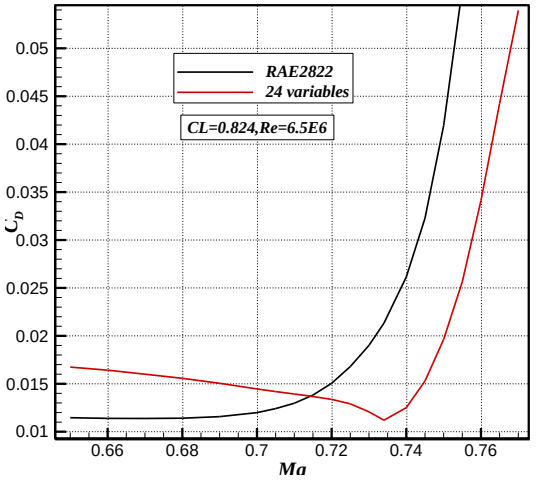

Fig. 4. The drag-divergence curves of initial and optimized airfoils.

3 The framework of RDO

A framework of RDO based on non-intrusive polynomial chaos expansion is built. The

framework includes three main parts, as shown in Fig. 5. The PCE coefficients are obtained by point collocation method (PCNIPC). The mathematic formulation of RDO about this case is defined in Eq. (2).

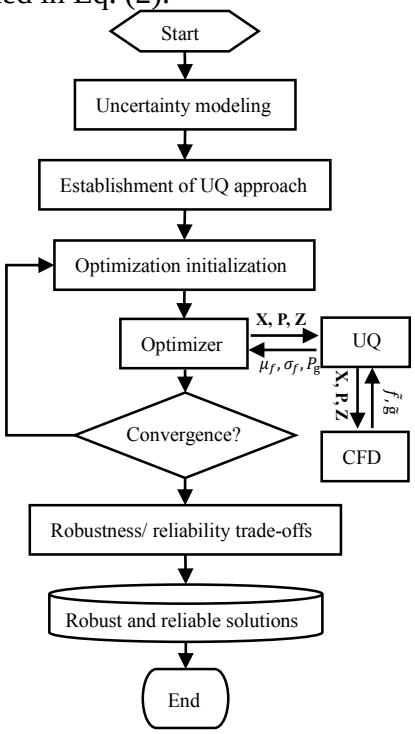

Fig. 5. General flowchart of RDO

$$\begin{aligned} &\mathrm{Re} = 6.5\times10^6, C_L = 0.824 \\ &Find \quad x \in R^d \\ &Min \quad \mu_{C_D} + \sigma_{C_D} \\ &S.t. \quad \mu_{C_m} - \sigma_{C_m} \geq -0.092, \\ &\quad Area \geq Initial(RAE2822), \\ &\quad Ma \sim (0.734, (0.02)^2), \end{aligned} \tag{2}$$

4 Establishment of sparse PC representation

4.1 Orthogonal matching pursuit

Sparse PC reconstruction can be regularized as l_1-minimization problem [6], also referred to as basis pursuit denoising (BPDN), as shown in

$$\min_{\boldsymbol{\beta}} \|\boldsymbol{\beta}\|_1, \ s.t. \|\boldsymbol{\psi}\boldsymbol{\beta} - \mathbf{Y}\|_2^2 \leq \varepsilon, \tag{3}$$

Eq. (3) can be solved by a large number of efficient algorithms. These algorithms include basis pursuit and greedy algorithms, e.g., OMP and least angle regressions (LARs) are widely used greedy algorithms.

OMP includes two important steps namely basis selection and coefficients update. Starting from initial active set $A^{(0)} = \phi$ and initial residual vector $\boldsymbol{\gamma}^{(0)} = \mathbf{Y}$, at each iteration k, OMP identifies only the most correlated basis with the current residual from the remaining set $\Omega - A^{(k)}$ namely chosen bases removed from the universal set Ω ,to be added to the active set. The residual vector $\boldsymbol{\gamma}^{(k+1)}$ is updated by subtracting the contribution of chosen bases of active set from the output vector. The iteration procedure is continued until the residual tolerance ε is achieved. The following depicts a step-by-step implementation of the OMP algorithm.

Table 2 Orthogonal matching pursuit algorithm

Algorithm1: OMP

Input: $\mathbf{Y} = \{y^{(j)}\}_{j=1}^N, \{\boldsymbol{\Xi}^{(j)} = (\xi_1^{(j)}, \xi_2^{(j)}, \cdots, \xi_n^{(j)})\}_{j=1}^N, \varepsilon > 0.$

Output: $A^{(k)}, \boldsymbol{\beta}^{(k)}$

Initialization: $k = 0, A^{(0)} = \phi, \boldsymbol{\gamma}^{(0)} = \mathbf{Y}, \Omega = \{1,2,\cdots M\},$
$\{\boldsymbol{\psi}_1, \boldsymbol{\psi}_2, \cdots, \boldsymbol{\psi}_M\} = \{\psi_i(\boldsymbol{\Xi}^{(j)})\}_{N\times M}$

While $k < M$ & $\|\boldsymbol{\gamma}^{(k)}\| \geq \varepsilon$ **do**

$i_+^{(k+1)} = \arg\max_i |\boldsymbol{\Psi}_i^T \boldsymbol{\gamma}^{(k)}| / \|\boldsymbol{\psi}_i\|_2 \ \ (i \in \Omega / A^{(k)})$

$A^{(k+1)} = A^{(k)} \cup \{i_+^{(k+1)}\}$

$\boldsymbol{\beta}^{(k+1)} = arg\min_{\boldsymbol{\beta}} \|\mathbf{Y} - \boldsymbol{\Psi}_{A^{(k+1)}}^T \boldsymbol{\beta}\|$

$\boldsymbol{\gamma}^{(k+1)} = \mathbf{Y} - \boldsymbol{\Psi}_{A^{(k+1)}}^T \boldsymbol{\beta}^{(k+1)}$

$k \leftarrow k + 1$

end while

4.2 Numerical example

A complex scalar function with two independent random inputs is formulated as

$$f(x_1, x_2) = \ln(1 + x_1^2)\sin 5x_2 \tag{4}$$

where x_1, x_2 are assumed to be normally distributed with the mean $\mu = 2.0$ and standard deviation $\sigma = 0.4$. We set standard normally distributed variables $\xi_i \in N(0, 1^2)$, and inputs can be expressed by $x_i = 2.0 + 0.4\xi_i, (i = 1,2)$. The reference values of mean (μ_f) and standard deviation (σ_f) are -0.115369 and 1.141393, respectively. Fig. 6 gives the true response of the two-dimensional function. To examine the performance of OMP, we estimate the stochastic performance of f by OMP algorithm and full PC representation, respectively. The convergence procedures of relative error of mean and standard deviation with increasing number of collocation points for the two methods are shown in Fig. 7 and Fig. 8, respectively. Their results show that OMP algorithm achieves the faster reduction rate of error than full PC metamodel. When the number of collocation points reaches 20, OMP achieves $O(10^{-1})$ and $O(10^{-2})$ magnitude for

relative error of mean and standard deviation, respectively. As a contrast, based on 20 collocation points, the relative error of mean and standard deviation by full PC are $O(10^0)$ and $O(10^0)$, respectively. Fig. 9 gives the comparisons of estimated PDF of building PC metamodel by OMP and full PC. The results show that sparse PC representations achieve more consistency with that by MCS than full PC. Hence, these results indicate that the OMP method can enhance the sparsity of PCE and achieve more accurate estimate of the stochastic behavior of a solution. On the other hand, the OMP method needs less number of collocation points compared with full PC when required the same prediction accuracy, largely improving the efficiency of probabilistic UQ.

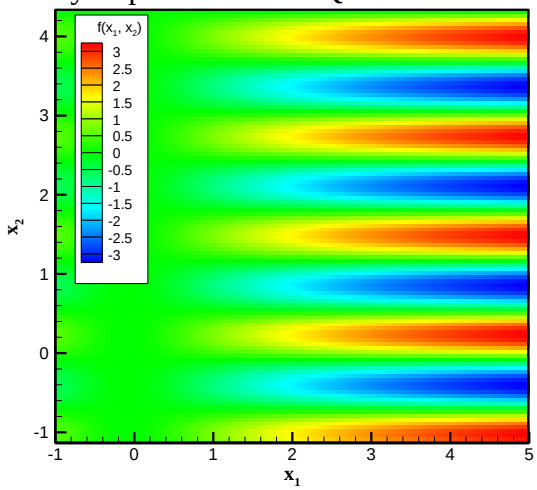

Fig. 6. True response of two-dimensional function

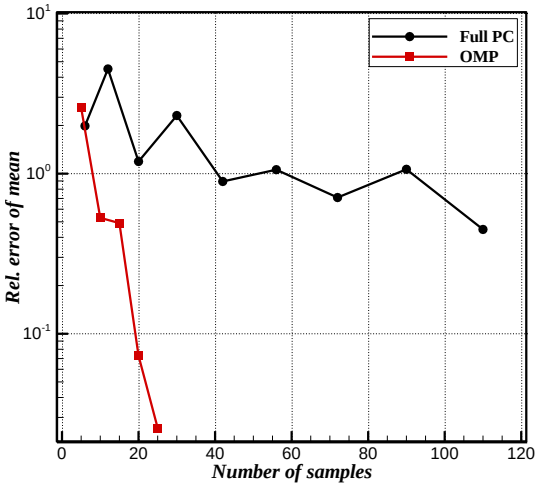

Fig. 7. The comparison of relative error in estimate mean

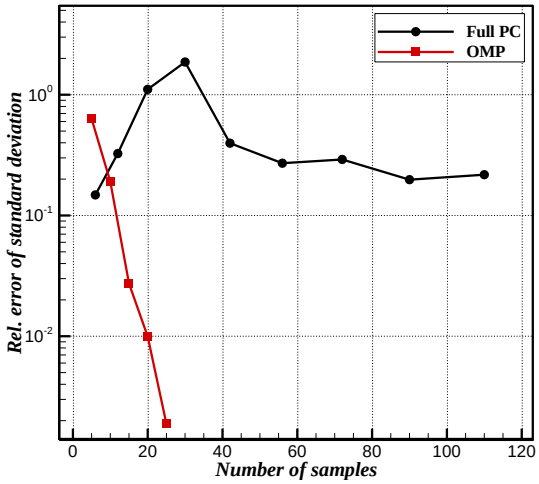

Fig. 8. The comparison of relative error in estimate standard deviation

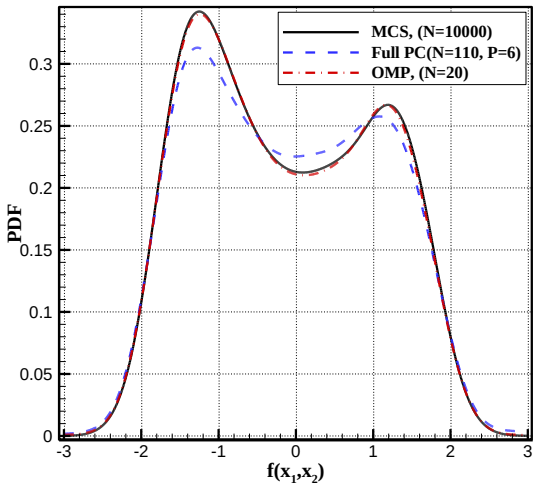

Fig. 9. The comparison of estimate PDF by OMP and full PC

5 Results and discussion

OPT1 and OPT2 are achieved by deterministic optimization (Eq. (1)) and robust optimization (Eq. (2)) respectively. OPT1 has smaller camber near 20% chord and larger camber near 80% chord compared with RAE2822 airfoil, while OPT2 holds smaller leading edge radius and larger camber near trailing edge compared with OPT1, as shown in Fig. 10. Fig. 11 shows that OPT1 smooths the shock while OPT2 has weak shocks occurring on its upper surface. Fig. 12 shows that a very weak shock occurs on the upper surface of OPT2 while a strong shock occurs on the upper surface of OPT1. As shown in Fig. 13, OPT1 reduces the drag only at the design point while OPT2 holds robust drag over a range of Mach numbers and improves the drag-divergence Mach number to 0.755. Table 3 gives

the aerodynamic results of initial and optimized airfoils. OPT1 and OPT2 achieve a drag reduction of 48.42% and 43.34% from the initial airfoil respectively at design point ($Ma = 0.734$, $Re = 6.5 \times 10^6$, $C_L = 0.824$). These results indicate that RDO provides an effective approach to circumventing the issue occurred in transonic airfoil optimization.

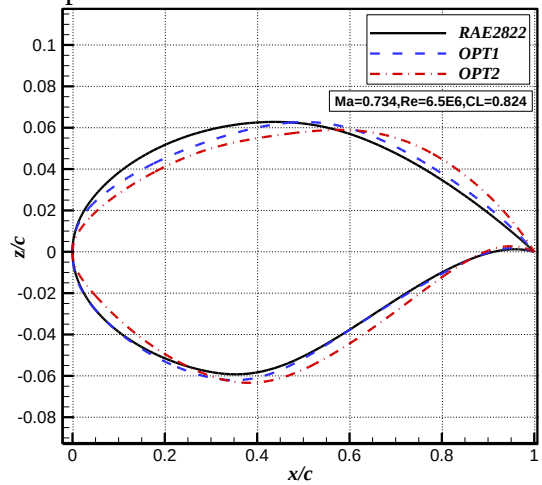

Fig. 10. Initial and optimized airfoils

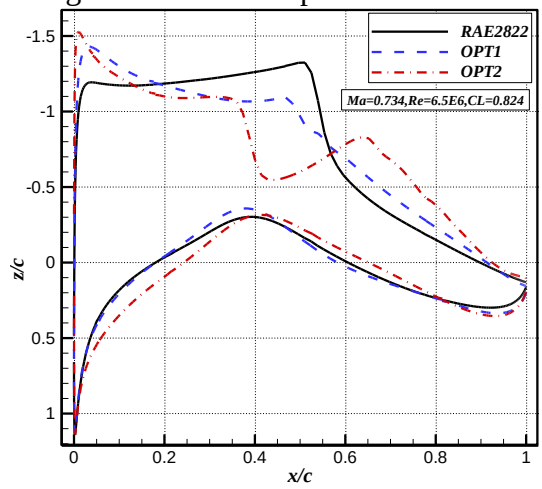

Fig. 11. Initial and optimized pressure distributions

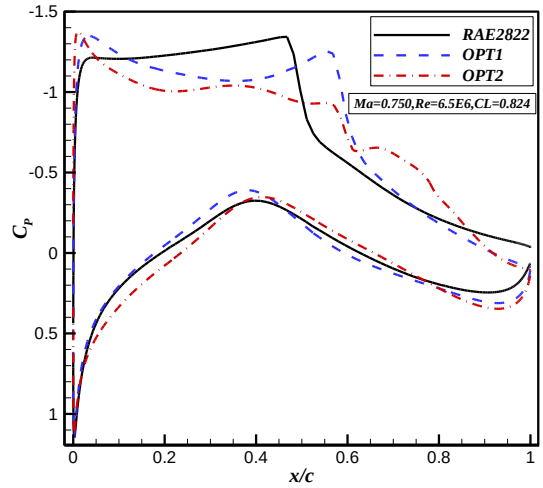

Fig. 12. Initial and optimized pressure distributions

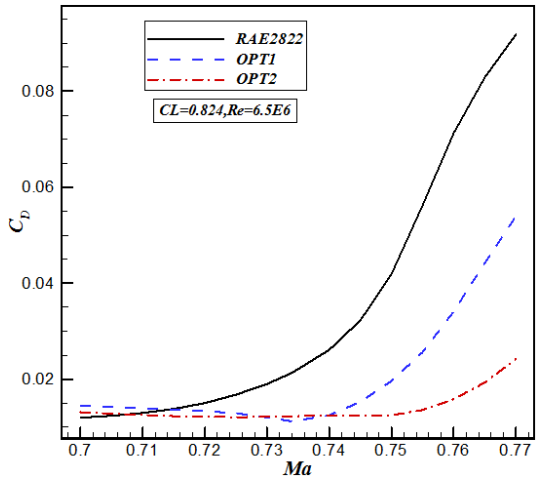

Fig. 13. Drag-divergence curves of initial and optimized airfoils

Table 3 The aerodynamic characteristics of initial and optimized airfoils at design point

Airfoil	C_D	C_m	Area	CFD runs
RAE2822	0.02171	-0.08743	0.077870	0
Deterministic design (OPT1, 24 variables)	0.01120	-0.08690	0.077918	1000
Robust design (OPT2, 24 variables)	0.01230	-0.09198	0.077880	1500

References

[1] Huan, Z., Zhenghong, G., Fang, X., and Yidian, Z. "Review of Robust Aerodynamic Design Optimization for Air Vehicles," *Archives of Computational Methods in Engineering*, pp. 1-48, 2018. doi: 10.1007/s11831-018-9259-2

[2] Padulo, M., Campobasso, M. S., and Guenov, M. D. "Comparative analysis of uncertainty propagation methods for robust engineering design," *International Conference on Engineering Design, ICED07*. Paris, France, pp. 1-12, 2007.

[3] Lee, S. H., and Chen, W. "A comparative study of uncertainty propagation methods for black-box-type problems," *Structural & Multidisciplinary Optimization* Vol. 37, No. 3, pp. 239-253, 2008.

[4] Zhao, H., Gao, Z. H., Gao, Y., and Wang, C. "Effective robust design of high lift NLF airfoil under multi-parameter uncertainty," *Aerospace Science and Technology* Vol. 68, pp. 530-542, 2017.

[5] Ledoux, S. T., Vassberg, J. C., Young, D. P., Fugal, S., Kamenetskiy, D., Huffman, W. P., Melvin, R. G., and Smith, M. F. "Study Based on the AIAA Aerodynamic Design Optimization Discussion Group Test Cases," *AIAA Journal* Vol. 53, No. 7, pp. 1-26, 2015.

[6] Rauhut, H., and Ward, R. "Sparse Legendre expansions via ℓ1-minimization," *Journal of Approximation Theory* Vol. 164, No. 5, pp. 517-533, 2012.

Contact Author Email Address

Corresponding author:
zgao@nwpu.edu.cn (Zhenghong Gao)
huanzhao_aero@163.com (Huan Zhao)

Copyright Statement